

Ultra-Flat Galaxies Selected from RFGC Catalog. I. The Sample Properties

V. E. Karachentseva,¹ Yu. N. Kudrya,² I. D. Karachentsev,^{3,*}
 D. I. Makarov,^{3,**} and O. V. Melnyk⁴

¹*Main Astronomical Observatory of National Academy of Sciences of Ukraine, Kiev, 03680 Ukraine*

²*Astronomical Observatory of Taras Shevchenko National University of Kiev, Kiev, 04053 Ukraine*

³*Special Astrophysical Observatory of the Russian AS, Nizhnij Arkhyz 369167, Russia*

⁴*Taras Shevchenko National University of Kiev, Kiev, 01033 Ukraine*

(Received October 27, 2015; Revised December 22, 2015)

We used the Revised Flat Galaxy Catalog (RFGC) to create a sample of ultra-flat galaxies (UFG) covering the whole northern and southern sky apart from the Milky Way zone. It contains 817 spiral galaxies seen edge-on, selected into the UFG sample according to their apparent axial ratios $(a/b)_B \geq 10.0$ and $(a/b)_R \geq 8.53$ in the blue and red bands, respectively. Within this basic sample we fixed an exemplary sample of 441 UFG galaxies having the radial velocities of $V_{LG} < 10000 \text{ km s}^{-1}$, Galactic latitude of $|b| > 10^\circ$ and the blue angular diameter of $a_B > 1'.0$. According to the Schmidt test the exemplary sample of 441 galaxies is characterized by about (80–90)% completeness, what is quite enough to study different properties of the ultra-flat galaxies. We found that more than 3/4 of UFGs have the morphological types within the narrow range of $T = 7 \pm 1$, i.e. the thinnest stellar disks occur among the Scd, Sd, and Sdm types. The average surface brightness of UFG galaxies tends to diminish towards the flattest bulge-less galaxies. Regularly shaped disks without signs of asymmetry make up about 2/3 both among all the RFGC galaxies, and the UFG sample objects. About 60% of ultra-flat galaxies can be referred to dynamically isolated objects, while 30% of them probably belong to the scattered associations (filaments, walls), and only about 10% of them are dynamically dominating galaxies with respect to their neighbours.

1. INTRODUCTION

In his study “The Classification of Spiral Galaxies” [1] Edwin Hubble, answering the criticisms of John Reynolds has re-designated the structural features that divide the spiral galaxies into the “early” (Sa), “intermediate” (Sb) and “late” (Sc) types. He called the relative size of the unresolved galactic nucleus (sign 1) the first and basic criterion, i.e. in the contemporary terminology—the size of the bulge with respect to the disk. By the time, only 290 images were used to classify the spirals, and hence, Hubble did not consider the axial ratio to be an essential criterium for the classification, as urged by Reynolds. Nevertheless, sign (1), along with the openness of the spiral structure (2) and the de-

gree of concentration of matter in the arms (3) formed a solid basis for Hubble’s statistical conclusions about the relationship of different characteristics of galaxies. In the same paper [1] Hubble did not agree with Reynolds’s assumption that the spirals, seen edge-on, should be classified in a separate class, according to the ratio of their axes and the absorption pattern in them.

A further elaboration and development of the Hubble sequence of galaxies is due mainly to the widely known studies of de Vaucouleurs and Sandage (see, e.g., the survey by Buta [2]). The class of the late Hubble spirals Sc got a natural extension for the “bulge-less” Scd, Sd, and Sm types for all the angles of inclination to the line of sight i . At that, as shown by Karachentsev [3], the galaxies, seen nearly edge-on ($i > 85^\circ$) are much easier to classify by the (reverse) “bulge/disk” ratio and isolate among them very thin purely disk spirals. As it was stressed by

* Electronic address: ikar@sao.ru

** Electronic address: dim@sao.ru

Kormendy and Kennicutt [4], ultra-thin spiral galaxies are of particular interest in light of their origin and survival in the environments of different density.

Flat galaxies were long known as spiral galaxies of late morphological types, seen edge-on, with a small or a missing nucleus [5, 6]. To date, a large number of observations of flat galaxies were conducted in the optical and radio ranges (see the survey of Kautsch [7]). However, a systematic catalogization of flat galaxies became possible only at the advent of homogeneous sky surveys, implementing certain selection conditions.

The first catalog of flat edge-on galaxies, the Flat Galaxy Catalog, FGC(E) and its updated RFGC version are published in [8, 9]. The RFGC catalog [9] covers the entire sky and contains 4236 galaxies, visually selected on the blue (further, B) and red (further, R) prints of the first Palomar sky survey POSS-I and the ESO/SERC survey, with the “blue”, in the POSS-I system, major axis $(a/b)_B \geq 7$ at the angular diameter (major axis) of $a_B \geq 0'.6$. Further, for brevity, we shall use the expressions “blue (red) diameter” and “blue (red) axial ratio”, referring to the diameter and the galaxy image axial ratio on the blue (red) print. The criterion of the axial ratio was later used as one of the main factors creating the catalogs of flat spiral galaxies: in the near infrared 2MASS range [10], in 2MFGC [11] and in different releases of the Sloan survey: SDSS DR1 [12] and SDSS DR7 [13].

In his review paper [7] Kautsch describes various models of formation and evolution of thin disks, the properties of such objects based on the data from the catalogs [8, 9, 12], as well as the results of observations of individual objects. The details can be found in the extensive list of references therein. Note that the choice of the apparent axial ratio criterion for ultra-thin galaxies by different authors is rather arbitrary (see the survey of observational data in [7]). For example, Goad and Roberts [14] give the results of spectroscopic observations for the galaxies with a/b in the range of 9–20 (the optical range).

The well-known “classical” super-thin isolated galaxy UGC 7321 = FGC 1403 = RFGC 2246 = 2MFGC 9681

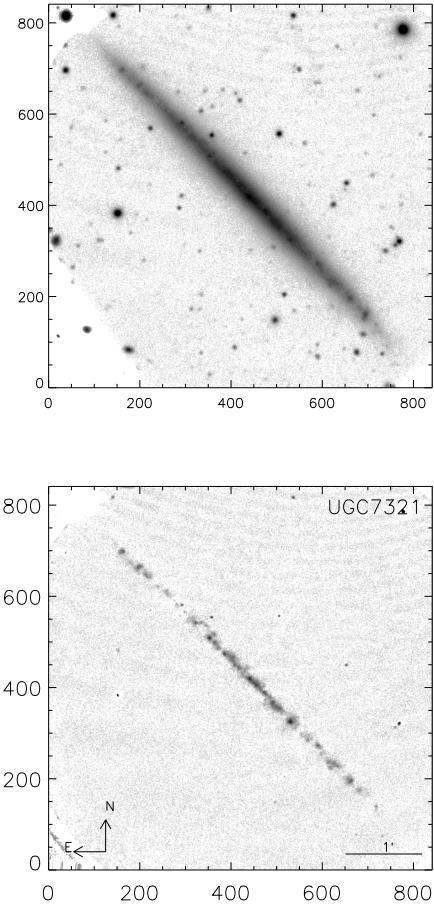


Figure 1. A pair of images of the UGC 7321 galaxy, obtained at the 6-meter BTA telescope with the SCORPIO focal reducer [17]. Top: an image in the continuum with the SED607+SED707 filters, $a/b = 14$. Bottom: an image in the line of $H\alpha$ with the subtraction of the continuum, $a/b = 38$. The scale and orientation are shown in the corners of the bottom image.

(KIG 524 [15] = 2MIG 1699 [16]) has an axial ratio of $(a/b)_B = 16$, $(a/b)_R = 13$ in the RFGC. Meanwhile, the $H\alpha$ line observations for the subsystem of the emission H II regions of this galaxy give the axial ratio of $(a/b)_{H\alpha} = 38$ (see Fig. 1).

These numbers show that the axial ratio of a galaxy depends on the color (age) of its stellar population. The flattest subsystem is formed by the youngest stars with the age of about 10 Myr, concentrated in the H II regions.

For all the galaxies in the FGC(E) catalog, the apparent axial ratio in the blue range does

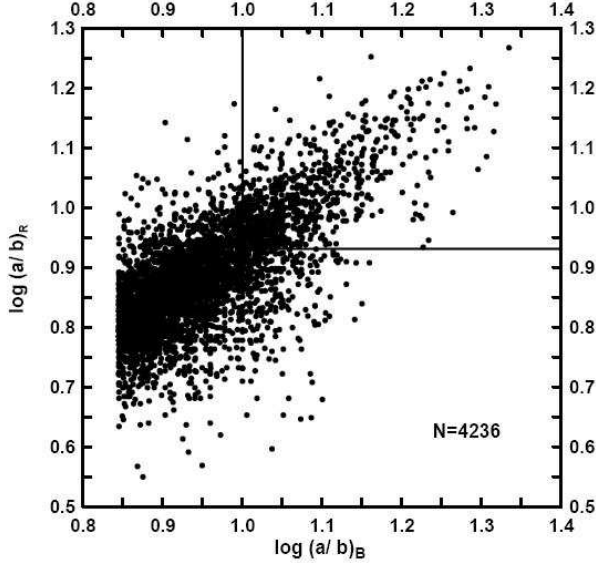


Figure 2. The distribution of RFGC galaxies by the red (R) and blue (B) axial ratios. The upper right corner contains the UFG galaxies, limited by the lines $(a/b)_B = 10$ and $(a/b)_R = 8.53$.

not exceed $(a/b)_B = 22.4$. It corresponds to the maximum value of true (spatial) axial ratio of 25.8 [18]. The latter value is of vital importance for the models of formation and stability of thin stellar disks.

The aim of this study is to create an exemplary sample of ultra-thin galaxies from the RFGC catalog and compare the presented properties of such objects, located in different environments. Section 2 briefly enumerates selection effects, affecting the image of a spiral galaxy seen edge-on, and describes the selection procedure of ultra-thin galaxies from the RFGC catalog. Section 3 shows the characteristics of ultra-thin galaxies compared with all the RFGC galaxies. In Section 4, we consider different ways of identifying the environment and compare the catalog properties of ultra-thin galaxies, located in different environments. Brief conclusions are given in Section 5.

2. A SAMPLE OF SUPER-THIN EDGE-ON SPIRAL GALAXIES

The distribution of the RFGC galaxies by the blue (B) and red (R) axial ratios is demonstrated in Fig. 2. As shown in [19], the lin-

ear regression between them has the shape of $(a/b)_R = 0.853(a/b)_B$ with a rather large dispersion. To sever the galaxies with prominent bulges, we chose the following conditions as a criterion for a super-thin (ultra-flat) galaxy (Ultra Flat Galaxies = UFG): $(a/b)_B \geq 10.0$ and $(a/b)_R \geq 8.53$ (the upper right corner of Fig. 2.)

Obviously, the statistics of the observed properties of ultra-thin galaxies selected this way is affected by various selection effects. Let us list the main ones:

- (1) In the remote/small/faint galaxies the axial ratio is determined, basically, by the size of the minor axis b , which is affected by the resolution of the photographic emulsion and the seeing. Thus, for a galaxy with $a = 36''$ and $a/b = 10$ the value amounts to $b = 3''.6$, which is comparable to the typical resolution on the photographs of the Palomar sky survey of about $3''$.
- (2) The amount of data on the radial velocities of distant, $V_{LG} > 10\,000\text{ km s}^{-1}$ galaxies rapidly decreases with increasing distance, hence, it becomes difficult to estimate the number of their natural satellites.
- (3) The shapes of the galaxies in the zone of the Milky Way, especially the edge-on late spirals are affected by the absorption in our own Galaxy, as well as the foreground stars.

The angular size distribution of the RFGC galaxies and the influence of the above-mentioned effects can well be seen on the panels of Fig. 3, where the “ $\log(b_B) - \log(a_B)$ ” and “ $\log(b_R) - \log(a_R)$ ” diagrams are presented to the left and right, respectively. A thin line on both panels is determined by the condition $a/b = 7$, i.e. $\log(b) = \log(a) - 0.845$. The following features are distinctly conspicuous: a) in red color the RFGC galaxies on the average look thicker than in blue color; b) the diameter dispersion increases with decreasing size of galaxies; c) at the value of $\log(b) \sim -1.3$ ($b \sim 3''$) the shortage of the number of galaxies becomes noticeable caused by the limit, resulting from the resolution of the photographic emulsion. For small-sized galaxies the measurement resolution

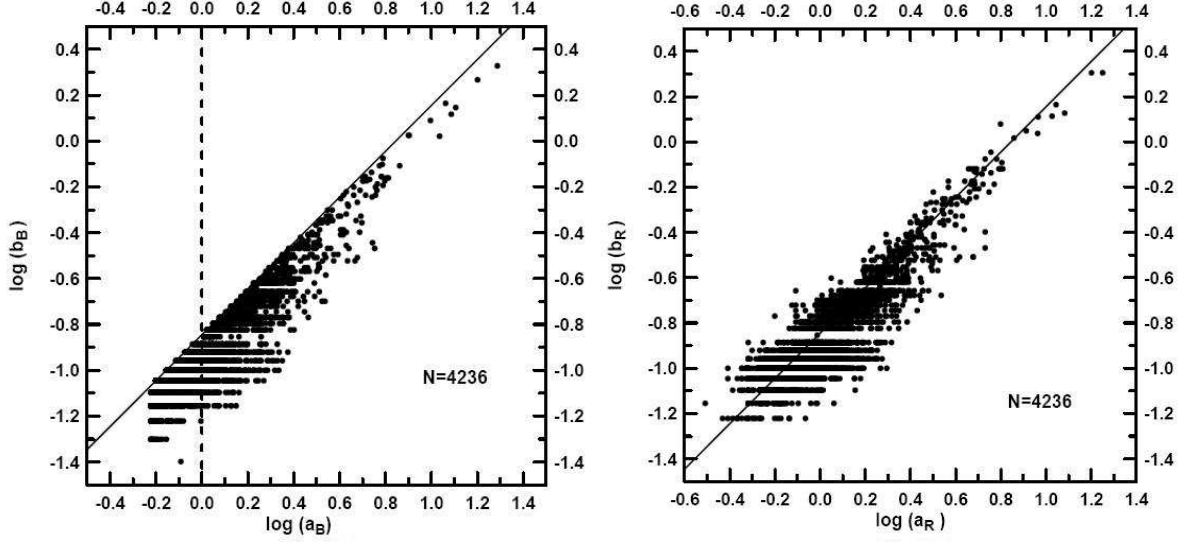


Figure 3. The left plot shows the distribution of 4236 flat galaxies of the RFGC catalog by the blue major and minor diameters $\log(b_B)$ vs. $\log(a_B)$ in minutes of arc. The thin line corresponds to the condition $(a/b)_B = 7$, i.e. $\log(b_B) = \log(a_B) - 0.845$. The dashed line is drawn for the value of $a_B = 1.0$. The right plot shows the distribution of 4236 RFGC flat galaxies by the red major and minor diameters $\log(b_R)$ from $\log(a_R)$. The thin line corresponds to the condition $(a/b)_R = 7$.

Table 1. The distribution of RFGC galaxies by the blue major diameters and radial velocities V_{LG}

$V_{LG}, \text{ km s}^{-1}$	$a_B \geq 2.0$	1.99–1.50	1.49–1.00	0.99–0.60	$a_B \geq 0.6$	$a_B \geq 1.0$
(0–1000]	4/35 (11)	2/11 (18)	0/5 (0)	0/5 (0)	6/56 (11)	6/51 (12)
(1000–2000]	16/69 (23)	9/27 (33)	5/23 (22)	3/22 (14)	33/141 (23)	30/119 (25)
(2000–3000]	20/79 (25)	7/36 (19)	7/57 (30)	3/28 (11)	47/200 (24)	44/172 (26)
(3000–4000]	12/38 (32)	16/47 (34)	19/61 (31)	3/36 (8)	50/182 (27)	47/146 (32)
(4000–5000]	14/39 (36)	14/65 (22)	39/125 (31)	8/53 (15)	75/282 (27)	67/229 (29)
(5000–6000]	12/33 (36)	15/53 (28)	40/129 (31)	8/65 (12)	75/280 (27)	77/215 (36)
(6000–7000]	9/24 (38)	14/36 (39)	41/117 (35)	6/108 (6)	70/285 (25)	64/177 (36)
(7000–8000]	5/14 (36)	8/34 (24)	31/89 (38)	6/99 (6)	50/236 (21)	44/137 (32)
(8000–9000]	3/6 (50)	12/26 (46)	30/90 (33)	4/92 (4)	49/214 (23)	45/122 (37)
(9000–10 000]	2/2 (100)	3/18 (17)	22/71 (31)	8/111 (7)	35/202 (17)	27/91 (30)
(0–10 000]	97/339 (29)	100/353 (28)	244/767 (32)	49/620 (8)	490/2078 (24)	441/1459 (30)
> 10 000	2	27	255	657	941	284
RFGC, with V_{LG}	341	380	1022	1277	3020	1743
All RFGC	343	384	1174	2335	4236	1901

of minor diameter is evident.

A simultaneous fulfillment of the conditions $(a/b)_B \geq 10.0$ and $(a/b)_R \geq 8.53$ isolates 19% of ultra-flat galaxies with the diameter of $a_B \geq 0.6$ from the entire RFGC catalog. We shall designate this sample of 817 galaxies the “base UFG.” Taking into account the above-mentioned selection effect we introduce additional restrictions: $V_{LG} \leq 10\,000 \text{ km s}^{-1}$, and galactic latitude $|b| > 10^\circ$. Four hundred and ninety objects satisfy the required criteria of ultra-thin galaxies (the “ $N = 490$ ” sample).

Table 1 gives a comparison of the two-dimensional distributions of the RFGC galaxies by the radial velocities in the Local Group system and the major blue angular diameters. We have adopted the radial velocity estimates from the NED¹ and HyperLeda² databases. The denominator contains the number of all the RFGC galaxies ($a_B \geq 0.6$, $(a/b)_B \geq 7$) with $V_{LG} \leq 10\,000 \text{ km s}^{-1}$ (this is the “ $N = 2078$ ” sam-

¹ www.ned.ipac.caltech.edu

² <http://leda.univ-lyon1.fr/>

ple), the numerator contains the number of all the ultra-thin galaxies, while the percentage of ultra-thin galaxies in the appropriate bin is in the brackets.

The data of Table 1 demonstrate a significant decrease in the fraction of ultra-thin galaxies with the angular diameters from 0.99 to 0.60 for all the radial velocity ranges. No significant difference is observed in the fraction of ultra-thin $N = 490$ sample galaxies in all the radial velocity ranges, except the first (with a small number of objects) and the last one. Recall that the statistics for the distant galaxies is affected by the selection effects noted above. Therefore, to achieve an acceptable completeness we select a yet more refined sample, $N = 441$ (the last column of Table 1) in which the $a_B \geq 1.0$ condition is fulfilled instead of $a_B \geq 0.6$. It amounts to about 10% of the total number of flat RFGC galaxies. Earlier, in [20] we found that the FGC(E) catalog itself is about 90% complete at $a_B \geq 1.0$. The data of Table 1 shows that the sample of ultra-thin galaxies is as well almost complete for the galaxies with the velocities of less than $10\,000\text{ km s}^{-1}$ exactly given $a_B \geq 1.0$.

The Schmidt test $\langle V/V_{max} \rangle$ [21] for the $N = 441$ sample is given in Fig. 4. For the maximum and initial angular diameter the values of 6' and 0.6 have been taken, respectively. It is evident that the completeness at the level of 80–90% is achieved at $a_{min} \sim 1.0$.

The Annex gives a list of RFGC numbers for 817 galaxies of the base UFG-sample. The RFGC-numbers of galaxies of the refined UFG-sample $N = 441$ are marked with two asterisks, 49 galaxies outside the UFG-sample, but included in the $N = 490$ sample, are marked with one asterisk.

Figure 5 gives the maps of sky distributions in the equatorial coordinates for the RFGC galaxies (points) and the UFG sample (filled circles). The gray watercolour wash designates the region of strong absorption near the Galactic equator $|b| \leq 10^\circ$. The following sections by the radial velocities are presented: $V_{LG} < 3000\text{ km s}^{-1}$, $3000 < V_{LG} < 10\,000\text{ km s}^{-1}$, $V_{LG} > 10\,000\text{ km s}^{-1}$, the radial velocities are not measured. The array of the images gives an idea of the relative positions of the UFG sample

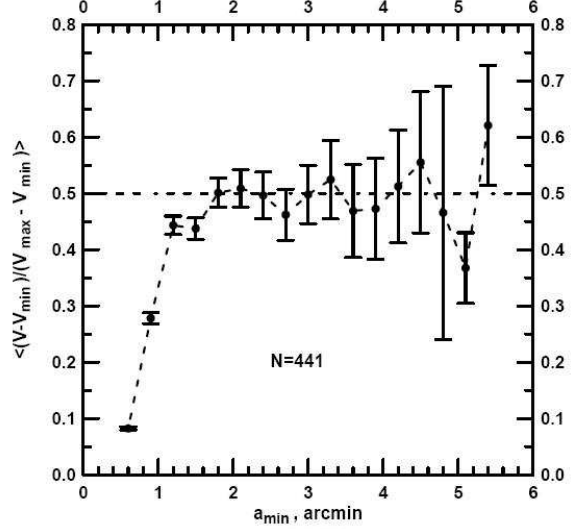


Figure 4. The Schmidt test for the $N = 441$ sample

objects and all the flat galaxies from the RFGC catalog at different depths.

On the top panel of Fig. 5 we can see that the nearby ultra-thin galaxies barely outline the Local Supercluster. An excess of UFGs in the region of the Local Supercluster center (RA = 12^h5, Dec = +12°) as compared to the homogeneous distribution is only $\Delta N \sim 5$ of galaxies. The section of $3000\text{--}10\,000\text{ km s}^{-1}$ (the second panel from the top) is filled the most complete mainly due to the observations with the 300-m Arecibo Observatory radio telescope [22], the 6-m BTA telescope [23] and the 100-m Radio Telescope Effelsberg [24, 25]. The galaxies in this radial velocity interval also show a barely discernible concentration in the regions of the well-known Coma and Pisces–Perseus clusters. Note that Fig. 5 and the data in Table 1 are highly complementary. This way, the two last lines of Table 1 for the galaxies with the angular diameters in the range of 0.60–0.99 show a noticeable lack of radial velocity measurements. Wherein an excessive localization of galaxies without radial velocities is observed in the southern hemisphere (the bottom panel).

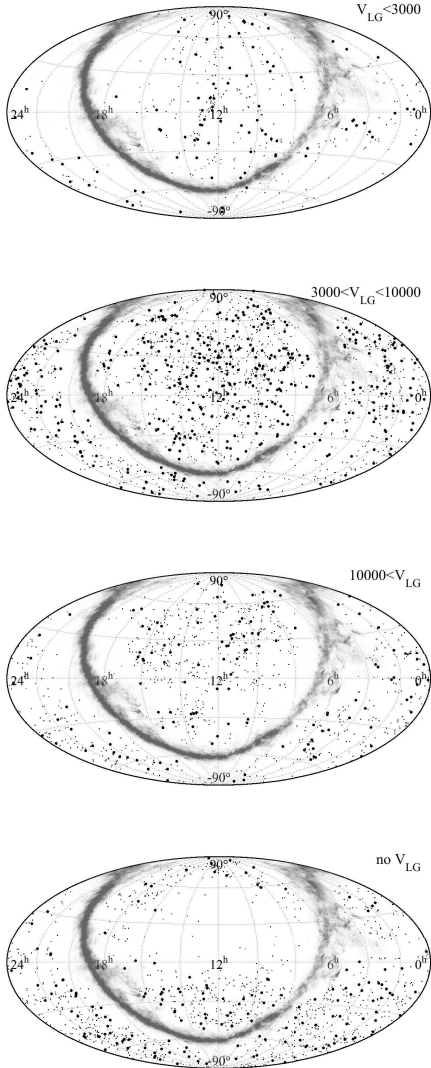


Figure 5. The maps of the sky distribution in the equatorial coordinates of the RFGC galaxies (points) and the UFG sample (filled circles). Gray watercolor wash designates the region of strong absorption near the Galactic equator $|b| \leq 10^\circ$. From top to bottom, the following sections by radial velocities are presented: $V_{LG} < 3000 \text{ km s}^{-1}$, $3000 < V_{LG} < 10\,000 \text{ km s}^{-1}$, $V_{LG} > 10\,000 \text{ km s}^{-1}$, and radial velocities are not measured.

3. THE PROPERTIES OF ULTRA-THIN GALAXIES COMPARED WITH THE RFGC GALAXIES

Among the 2078 galaxies of the RFGC catalog with radial velocities $V_{LG} < 10\,000 \text{ km s}^{-1}$, the average radial velocity in the Local Group

rest frame amounts to $5553 \pm 54 \text{ km s}^{-1}$. For the UFG sample of galaxies with angular diameters exceeding $0'.6$ ($N = 490$) and $1'.0$ ($N = 441$), the average velocity value is $5438 \pm 104 \text{ km s}^{-1}$ and $5366 \pm 110 \text{ km s}^{-1}$, respectively. This means that all the three samples insignificantly differ in depth.

Table 2 shows the distribution of galaxies by the morphological types of spirals in the initial RFGC catalog, in the sample of ultra-thin galaxies, and in the RFGC and UFG samples with measured velocities. The last two rows of Table 2 give the percentage of the ultra-thin galaxy sample objects in the corresponding bins. The first line contains the designations of the spiral types in the Hubble system, the second line—in the de Vaucouleurs digital system. As it was shown in [19], our estimates of different types vary from the digital estimates of de Vaucouleurs on the average by not more than ± 1 . In the same paper [19] it was noted that the RFGC galaxies show no dependence of the apparent axis ratio (or type) on the radial velocity up to values of about $10\,000\text{--}12\,000 \text{ km s}^{-1}$. As follows from the Table 2 data, the peak number of galaxies for the entire catalog, as well as the $N = 2078$ sample falls on the Sc type. For the UFG $N = 817$ and $N = 441$ samples the peak shifts to the Sd type, both in the general and in the fraction distributions. The fraction of ultra-thin galaxies rapidly decreases from the Sd type to later Sdm and Sm types, since turbulent motions play a significant role in the dynamics of the latter. As we can see, the morphological types of 80% of UFG-galaxies lie in the narrow range of $T = 7 \pm 1$. This is consistent with the result of [6]: the thinnest stellar disks are found in the galaxies classified as Scd, Sd, Sdm.

The surface brightnesses for the RFGC galaxies were estimated visually and were divided by the average surface brightness index SB: I, II, III and IV (where the class I galaxies have the highest surface brightness). Table 3 shows the distribution of the number of flat RFGC galaxies, the $N = 2078$ and $N = 441$ samples by the surface brightness class SB. The maximum in the distributions of 55–63% for all the samples falls on SB = II (what corresponds to about $25.4 \text{ mag/arcsec}^2$ in the B -band [8]). The last

Table 2. The distribution of RFGC galaxies and ultra-flat galaxies by the type of spirals

Type	Sab	Sb	Sbc	Sc	Scd	Sd	Sdm	Sm	All
T	2	3	4	5	6	7	8	9	—
RFGC	1	151	573	1535	960	718	252	37	4236
$N = 2078$	8	82	266	544	490	465	195	28	2078
UFG, $N = 817$	0	11	31	252	211	270	40	2	817
UFG, $N = 441$	0	9	17	81	109	188	35	2	441
N817/NRFGC,%	7	5	16	22	38	16	5	19	
N441/N2078,%	11	6	15	22	40	18	7	21	

Table 3. The distribution of RFGC galaxies and super-thin galaxies by the mean surface brightness index, SB

SB	I	II	III	IV	All
RFGC	242	2480	1369	145	4236
$N = 2078$	190	1306	534	48	2078
UFG, $N = 817$	23	451	310	33	817
UFG, $N = 441$	22	268	139	12	441
N817/NRFGC,%	10	18	23	23	19
N441/N2078,%	12	20	26	25	21

Table 4. The distribution of RFGC galaxies and super-thin galaxies by the asymmetry index, As

As	0	1	2	All
RFGC	2830	1159	247	4236
$N = 2078$	1260	640	178	2078
UFG, $N = 817$	568	209	40	817
UFG, $N = 441$	272	135	34	441
N817/NRFGC,%	20	18	16	19
N441/N2078,%	22	21	19	21

two rows of Table 3 specify the percentage of UFG galaxies among the RFGC-galaxies of each SB class with and without radial velocity measurements. These data show that there has been a decrease in the fraction of high surface brightness objects in the transition from flat RFGC-galaxies to ultra-flat UFGs. This trend corresponds to the expected dropout of galaxies with small bulges (Sbc type) compiling the UFG sample. In other words, in the transition from flat to ultra-flat galaxies there is a shift of the SB index towards faint surface brightness, SB = III, IV (or about 25.6–25.9 mag/arcsec² [8]).

Thus, a typical super-thin galaxy is a Sd-type spiral galaxy with low surface brightness. The diminished surface brightness can be caused by a stronger absorption of light in the ultra-thin

galaxies seen strictly edge-on, or rather by the lower density of their stellar disks.

The asymmetry of shape of a flat galaxy is quite difficult to estimate without a deep enough surface photometry. Hence the results given in Table 4 should be evaluated as preliminary. The shape asymmetry was characterized in the RFGC catalog as the As index, which took the values 0, 1 and 2 for the regular, intermediate and clearly disturbed forms, respectively. As we can see from the table data, flat galaxies of regular shapes make up from 62 to 70% and the most asymmetric—from 5 to 8% both throughout the catalog, and in the individual samples. It also follows from the data in Table 4 that the proportion of ultra-thin galaxies of different types of asymmetry among the $N = 2078$ sample of galaxies is about 20%, showing a slight tendency to decrease from regular to intermediate and disturbed shapes.

Therefore, our data shows no distinct relationship between the relative thickness of the stellar disk of a spiral galaxy and the degree of perturbations of its periphery.

4. THE PROPERTIES OF ULTRA-THIN GALAXIES DEPENDING ON THEIR ENVIRONMENT

We determined the density of the environment in several ways.

(1) In the RFGC catalog for each galaxy with the a_B diameter significant neighbors with angular diameters in the range of $[a_B/2 - 2a_B]$, located in a circle of $R = 10a_B$ radius were counted. At that, the neighbors were identified the same way for all the galaxies. By the time of the catalog publication, the data on the radial

velocities of RFGC galaxies and especially their fainter neighbors were very scarce. Therefore, the given numbers of neighbors in the projection give an idea only on the surface density of the background around the RFGC galaxies not accounting for its depth. Figure 6 demonstrates the histograms of distribution of the galaxies from four samples: RFGC, $N = 2078$, $N = 490$ and $N = 441$ by the number of significant neighbors. The right-hand side scale in each panel indicates the percentage of galaxies in the corresponding sample with the designated number of neighbors in the projection. The behavior of the distribution is about the same for the considered samples, and only 2–5% of the galaxies in each sample and in the entire RFGC catalog have more than three neighbors. As follows from the data in Fig. 6, there is a slight upward trend in the proportion of isolated galaxies in the transition from flat to ultra-flat galaxies.

(2) For each super-thin galaxy of the UFG samples we determined the number of galaxies with relative radial velocities in the range of $+500$, -500 km s^{-1} to the limiting projection distance of $R = 750$ kpc. Unlike in the previous case, radial velocities of galaxies were taken into account here. However, the neighbors, as in selection (1) can not reliably form physical systems with the UFG sample galaxies, although they share with them a fairly well-indicated general field by the velocities and distances.

The distribution of ultra-thin galaxies by the number of such neighbors for the $N = 490$ and $N = 441$ samples is shown in panels of Fig. 7 to the left and right, respectively. The left-hand side scale in the panels shows the number of galaxies in the bin, while the right-hand side scale indicates their percentage. The last value on both panels corresponds to the cases of seventeen or more neighbors.

We can see from the data of Fig. 7 that only a third (31%) of ultra-thin galaxies have no neighbors within this range of radial velocities and projection distances. This value is smaller than the proportion of isolated galaxies, 56%, taking the neighbors into account by method (1). It should be noted, however, that not all the neighbors with the velocities in the range of $+500$, -500 km s^{-1} and projection distances of

$R < 750$ kpc are the natural companions of ultra-flat galaxies. Some of them may belong together with the UFGs to the diffuse elements of the large-scale structure (filaments and walls).

(3) To all the galaxies with radial velocities below $20\,000$ km s^{-1} in the HyperLeda database at the galactic latitude of $|b| > 10^\circ$ the clustering algorithm, described in detail in [26, 27] was applied. Uniting the galaxies into systems of different populations, individual characteristics of all the galaxies were used, namely, their radial velocities, projected separations and masses determined by the integral infrared luminosity in the infrared K_s -band. Initially, we isolated physical pairs satisfying the conditions of the full negative energy, and pair location within the “zero velocity” sphere [28]. Then all the pairs with any common component were combined into a group. Eventually we had the data for the entire sky on the groups of galaxies and their environment up to $10\,000$ km s^{-1} . The resulting catalog was used for the analysis of the environment of galaxies of the RFGC catalog and the $N = 490$ and $N = 441$ samples. In this paper we used the following statuses to describe the environment: “isol” for isolated galaxies, “root” for the main member of the group, “mem” for a member of the group. Hence, method (3) gives a more accurate representation of the physical environment of ultra-thin galaxies than method (2), and the more so method (1).

For the $N = 490$ and $N = 441$ samples, we determined the frequency of galaxy occurrence in different environments. We considered the cases of selection by method (3) with the “isol,” “root” and “mem” status of a galaxy, as well as by method (2), when a galaxy has 0, 1, and 2 or more neighbors. The results are presented in Table 5. As follows from these data, more than 60% of ultra-thin galaxies belong to the category of dynamically isolated objects, about 30% are nonprincipal members of scattered groups (associations, filaments or walls) and only the tenth of them are classified as dynamically dominant objects with respect to their nearest neighbors. The numbers in three right-hand side columns of Table 5 are consistent with the data of Fig. 6 showing that more than a half of UFG galaxies, which have no neighbors by the selection method (2) are in fact dynamically isolated objects.

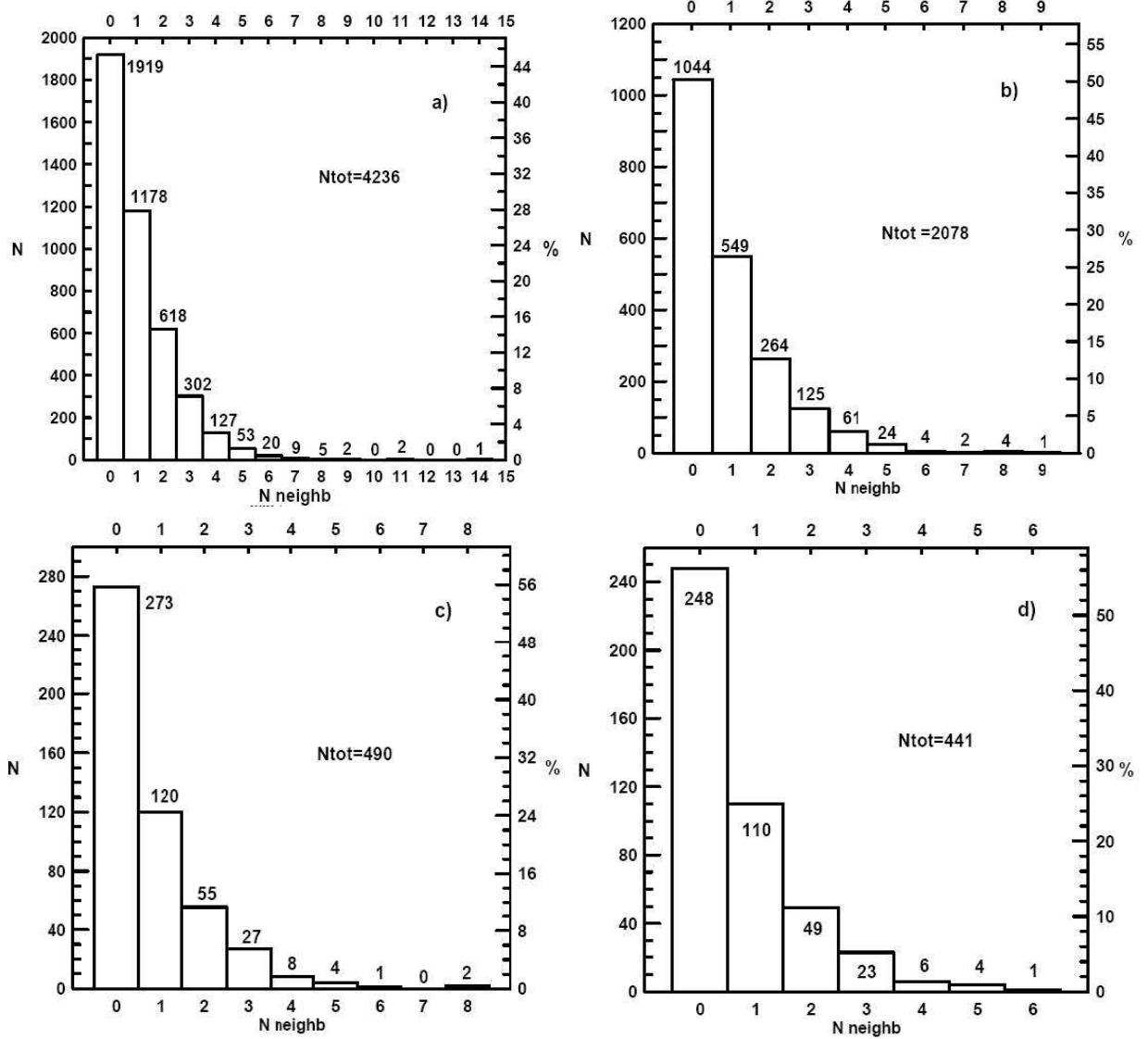


Figure 6. The distribution of flat galaxies by the number of significant neighbors with angular diameters in the range of $[a_B/2 - 2a_B]$ in a circle of $R = 10a_B$ radius for: (a) the entire RFGC catalog, (b) the RFGC sample with radial velocities below $10\,000\text{ km s}^{-1}$, $N = 2078$, (c) sample of ultra-thin galaxies with $a_B \geq 0.6$, $N = 490$, (d) sample of ultra-thin galaxies with $a_B \geq 1.0$.

Table 5. The occurrence of super-thin galaxies in different dynamic environments

Number	isol	root	mem	neighbors		
				0	1	≥ 2
$N = 490$	303	43	144	273	120	97
%	62 ± 4	9 ± 2	29 ± 3	56 ± 4	24 ± 3	20 ± 2
$N = 441$	267	41	133	248	110	83
%	61 ± 4	9 ± 2	30 ± 3	56 ± 4	25 ± 3	19 ± 2

Analyzing the average characteristics of ultra-flat galaxies relating to the categories “isol,” “root” and “mem,” we have noted the following

trends. The isolated ultra-thin galaxies on the average have a later morphological type. The dimmest average surface brightness is typical of isolated UFG galaxies. The degree of asymmetry of an ultra-flat galaxy reveals a positive correlation with the number of its neighbors.

5. DISCUSSION AND SUMMARY

Among the 4236 flat galaxies of the RFGC catalog [9], in which, by definition, the blue axial

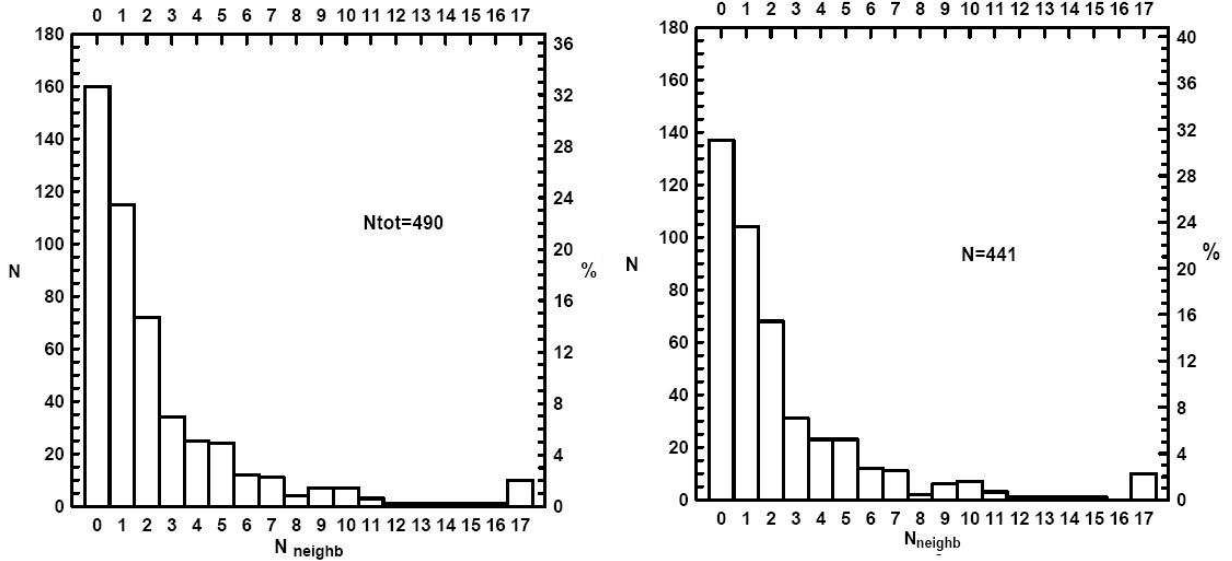


Figure 7. The distribution of ultra-thin galaxies by the number of neighbors up to the limiting projection distance of $R = 750$ kpc and with the radial velocities of V_{LG} over the range of $+500, -500$ km s^{-1} ; the $N = 490$ sample (left), the $N = 441$ sample (right).

ratios satisfy the relation $(a/b)_B \geq 7.0$, we have selected a sample of ultra-flat spiral galaxies, Ultra Flat Galaxies, UFG. This sample covers the entire northern and southern sky (except for the zone of the Milky Way) and comprises 817 galaxies with blue and red axial ratios $(a/b)_B \geq 10.0$ and $(a/b)_R \geq 8.53$, respectively. Within this initial (base) sample of ultra-thin spirals seen edge-on, we fix a refined sample of 441 UFG galaxies, satisfying the following conditions: radial velocity of the galaxy $V_{LG} < 10000$ km s^{-1} , Galactic latitude $|b| > 10^\circ$, the major angular diameter $a_B \geq 1'.0$. According to the Schmidt test, a list of 441 UFG galaxies, designated as (**) in the Annex, is approximately 80–90% complete and can serve as a model sample for the analysis of various characteristics of ultra-flat galaxies.

We notice UGC 7321=RFGC 2246 as a prototype of UFG-galaxies. This is an isolated spiral with a blue and red axial ratio of 16 and 13 respectively. On the $H\alpha$ -line image from [17] a subsystem of young (about 10 Myr) stars, immersed in the H II regions, has an apparent axial ratio of $(a/b)_{H\alpha} = 38$, which is the highest value among the flat galaxies. It is known that ultra-thin disks of galaxies are mainly found in the low number-density regions of the surrounding galaxies. We have estimated the density of the UFG

environment in three different ways.

- (1) In the RFGC catalog for each galaxy with the a_B diameter, significant neighbors with the angular diameters in the range of $a_B/2$ – $2a_B$, located in a circle of $R = 10a_B$ radius were counted.
- (2) The number of galaxies with relative radial velocities in the range of $+500, -500$ km s^{-1} to the projected linear distance of $R = 750$ kpc was determined.
- (3) The environment density was determined by the clustering method.

A comparison of the UFG list galaxies with the objects of the entire RFGC catalog allows us to draw the following conclusions.

- (a) More than 3/4 of UFG galaxies have their morphological types in a narrow range of values $T = 7 \pm 1$. In other words, the thinnest stellar disks are found in the galaxies that are classified as Scd, Sd, Sdm. This conclusion is in direct correspondence with the previous results of Heidmann et al. [6].
- (b) There appears a trend of diminishing average surface brightness in ultra-thin galaxies in the transition from the RFGC to the UFG sample. It is mainly due to the elution of the

Sbc-type galaxies with small bulges from the UFG sample. The other probable reason could be a stronger internal absorption of light in the ultra-thin galaxies seen edge-on.

(c) Regularly shaped disks of galaxies with no signs of asymmetry (disturbances) make up about 2/3 both in the main RFGC catalog and in the UFG sample. We observe only a slight tendency to an increase in the relative number of undisturbed shapes in super-thin galaxies. In general, the thickness of the stellar disk of a spiral galaxy is not related to the degree of disturbance (asymmetry) of its periphery.

(d) Using different methods of estimating the surrounding density of the UFG and RFGC galaxies, we have shown that the relative number of isolated galaxies depends on the apparent axis ratio of the stellar disk only marginally. According to our preliminary estimates, about

60% of ultra-flat galaxies can be classified as dynamically isolated objects, about 30% of them are part of the scattered associations (filaments and walls), and only about 10% of them are dynamically dominant object relative to their nearest neighbors.

In the following publications of this series we suggest to consider the integral (optical and radio) properties of ultra-flat spiral galaxies, and make the mass estimates of the dark haloes, enveloping the disks of UFG galaxies.

ACKNOWLEDGMENTS

The NED and HyperLeda databases were used in the study. IDK, DIM are grateful to the Russian Science Foundation (grant 14-12-00965) for the financial support of the study.

ANNEX

The list of RFGC numbers for 817 galaxies of the base sample. The catalog RFGC-numbers of galaxies from the $N = 490$ sample are marked by one asterisk (*). The catalog RFGC-numbers of galaxies from the $N = 441$ sample are marked by an additional asterisk and are listed in the base sample as (**).

1**	6**	16	18	25	31	34**	46	58	73**	81	88	96
99**	106	113**	119**	122**	123	124**	132	136**	155	161**	164**	166**
175	176**	187	193**	195	207**	210	213**	225**	229	234**	237**	239**
248	255**	261**	267	278**	282**	283	292	296**	300	301	302**	321
322	325	330**	333	337	342**	344**	357**	365**	368	371**	374**	377
381*	385**	389**	392	393	403	415	430*	433	438**	446**	461	463**
465**	467**	483	484**	485**	486	493	500*	504**	505**	509**	510**	511**
512	513	517**	523	527	529	531**	537	539	542	544**	557	560**
569	598**	603**	604**	615	620**	622**	625**	626**	627**	631	634**	642
653**	660	666	674**	676**	679	687**	693**	695**	697**	701	705	719**
720	722**	730	744**	746**	754	756**	766**	768	769**	772	778**	793
798**	809*	813	826**	827	828*	831	835	844*	849**	854	855**	858**
863	869*	871	877**	880	888**	900**	903**	911**	912*	925**	928	934
940	942	944**	946	950	972	975	979	988**	990	995	1000**	1005
1010	1013	1015*	1016	1021	1029*	1045	1046	1050	1051**	1055**	1059	1065
1083	1091**	1094	1095**	1099**	1107	1109**	1112**	1113*	1114**	1124	1129	1132**
1133**	1135**	1140**	1143**	1147**	1148	1149**	1150	1155	1157	1162	1169	1170
1171	1172**	1184**	1189*	1195**	1196**	1200**	1201	1211**	1231**	1234	1236**	1248**

1256	1259**	1275	1277**	1278	1284	1285*	1291**	1293**	1298**	1300**	1305	1313*
1322**	1325**	1329**	1333	1339**	1344	1346*	1348**	1355	1357	1358	1359**	1362*
1363	1365**	1366**	1374	1375**	1383**	1384*	1385	1387**	1392	1394**	1399**	1406
1407	1412	1413	1417**	1420**	1424	1425**	1433	1434**	1435**	1439**	1440**	1443**
1446**	1461*	1462**	1468**	1470**	1486**	1490**	1502**	1504**	1514**	1522**	1527**	1530**
1549	1551	1552	1553**	1555**	1556**	1560**	1561**	1562	1563	1567**	1568**	1569**
1572	1587**	1595**	1596	1597	1607	1620**	1625**	1626**	1627**	1630**	1636	1637
1646**	1648	1650**	1660**	1664	1670**	1672**	1674*	1685**	1687	1691**	1692**	1696*
1700**	1710**	1716**	1737	1739**	1742	1744**	1745	1753**	1761**	1766**	1771	1778
1782**	1783	1785	1789**	1791**	1795**	1796**	1807	1823	1834	1837*	1843	1845
1847	1864**	1871**	1874**	1880**	1886	1888**	1892**	1918	1925**	1936**	1940**	1943
1951	1952	1953	1957*	1958**	1959**	1973	1976**	1979**	1992	1993**	1996	2000**
2002**	2004	2005	2006**	2010**	2014*	2020**	2021**	2026**	2030	2035**	2037**	2039
2041	2042**	2045	2046	2048*	2050**	2051**	2053	2057**	2058	2061**	2067**	2069**
2077**	2078	2079**	2085**	2106**	2108	2111**	2118	2123	2126**	2127**	2129**	2132**
2145**	2146**	2148**	2156**	2158*	2165**	2173**	2175	2186	2187	2195*	2206**	2207
2210**	2211	2218**	2233**	2243	2246**	2250**	2253**	2259**	2260**	2266**	2283*	2290**
2295**	2297**	2301	2308**	2317**	2320**	2322**	2327**	2333**	2339**	2341	2347	2350
2357**	2361**	2368**	2378**	2380**	2382**	2387**	2392	2396	2398	2399**	2403	2415**
2421**	2428**	2429**	2430**	2443**	2446**	2450	2453**	2459**	2461*	2467**	2468**	2474**
2482	2496**	2506	2510	2523**	2524**	2526**	2531**	2546**	2548*	2549**	2550	2551**
2553	2555**	2556	2569**	2580**	2581**	2585	2590**	2592*	2597	2605	2611**	2617**
2623**	2631**	2635**	2637	2642	2652**	2668**	2676	2687**	2694**	2699**	2702**	2705**
2714	2716	2725**	2727	2736*	2740	2750*	2751	2752*	2755*	2757**	2768**	2774**
2779*	2785*	2791	2795**	2802**	2803**	2805**	2808*	2811**	2819**	2821	2834	2842
2843	2853**	2855	2864**	2872**	2875**	2876	2881	2885**	2886**	2897**	2898	2901**
2905	2906**	2908**	2918**	2919	2923**	2927**	2928**	2929	2931**	2932	2953	2965
2966**	2968	2969**	2979	2988**	2999*	3001	3007**	3008	3013	3027**	3032	3034
3036**	3037**	3044**	3046**	3054**	3064	3069	3076	3077	3078	3079	3080	3081**
3082	3087**	3094**	3095**	3097**	3103	3118**	3119	3125	3126	3129	3132**	3140
3153*	3158	3160**	3164**	3170	3172	3184	3185**	3186**	3190**	3198	3200	3208
3212**	3218**	3219**	3232**	3243**	3245	3256	3258**	3262**	3274**	3277**	3285**	3289**
3296	3297**	3304**	3316**	3322	3326	3331**	3337**	3350	3354	3356**	3359**	3364*
3365**	3367**	3371	3372	3377**	3378**	3383	3385**	3397	3400	3405**	3414**	3424
3431	3437**	3438	3439	3444**	3452	3465**	3468	3481**	3488	3489**	3491**	3515**
3516	3517	3518	3519**	3520**	3521	3522	3526	3527**	3532**	3534	3540	3555
3558	3561**	3563	3575**	3580**	3582	3587	3596	3598	3600**	3601	3603	3608**
3611	3619	3622*	3628	3631**	3636	3643**	3644**	3645**	3651**	3659*	3672	3684*
3686	3689	3697	3699**	3703	3707	3712**	3715	3723**	3727**	3729	3740	3750
3752*	3753**	3761	3769	3779	3783	3792**	3798	3803**	3804	3820**	3822	3824**
3827**	3828**	3833**	3846**	3854**	3856	3858**	3879**	3880**	3896**	3901	3915**	3919
3924	3928*	3930	3935**	3952**	3953**	3968	3975	3977**	3984*	3986**	3998**	4003
4010	4013**	4025**	4028**	4032**	4039**	4046	4053*	4054	4057**	4066**	4072**	4073
4074**	4076**	4078**	4080**	4081**	4091**	4101	4106**	4113**	4119**	4123*	4131	4134**
4137	4149**	4151	4163**	4172	4190**	4199	4203**	4209**	4214*	4230		

-
1. E. Hubble, Observatory **50**, 276 (1927).
 2. R. Buta, in: *Proc. Conf. on The World of Galaxies, Paris, France, 1988*, Ed. by H. G. Corwin and L. Bottinelli (Springer-Verlag, New York, 1989), p.29.
 3. I. Karachentsev, Astronom. J. **97**, 1566 (1989).
 4. J. Kormendy and R. C. Kennicutt, Annu. Rev. Astronom. Astrophys. **42**, 603 (2004).
 5. B. A. Vorontsov-Vel'yaminov, Sov. Astron. **17**, 452 (1974).
 6. J. Heidmann, N. Heidmann, and G. de Vaucouleurs, Mem. R. Astr. Soc. **75**, 85 (1972).
 7. S. J. Kautsch, Publ. Astronom. Soc. Pacific **121**, 1297 (2009).
 8. I. D. Karachentsev, V. E. Karachentseva, and S. L. Parnovskij, Astronomische Nachrichten **314**, 97 (1993).
 9. I. D. Karachentsev, V. E. Karachentseva, Yu. N. Kudrya, et al., Astrophysical Bulletin **47**, 5 (1999).
 10. T. H. Jarrett, T. Chester, R. Cutri, et al., Astronom. J. **125**, 525 (2000).
 11. S. N. Mitronova, I. D. Karachentsev, V. E. Karachentseva, et al., Astrophysical Bulletin **57**, 5 (2004).
 12. S. J. Kautsch, E. K. Grebel, F. D. Barrazza, and J. S. Gallagher, Astronom. and Astrophys. **445**, 765 (2006).
 13. D. V. Bizyaev, S. J. Kautsch, A. V. Mosenkov, et al., Astrophys. J. **787**, 24 (2014).
 14. J. W. Goad and M. S. Roberts, Astrophys. J. **250**, 79 (1981).
 15. V. E. Karachentseva, Communications Spec. Astrophys. Obs., No. 8, 3 (1973).
 16. V. E. Karachentseva, S. N. Mitronova, O. V. Melnyk, and I. D. Karachentsev, Astrophysical Bulletin **65**, 1 (2010).
 17. I. D. Karachentsev, S. S. Kaisin, and E. I. Kaisina, Astrophysics **58**, 453 (2015).
 18. Yu. N. Kudrya, I. D. Karachentsev, V. E. Karachentseva, and S. L. Parnovskii, Astronomy Letters **20**, 8 (1994).
 19. I. D. Karachentsev, V. E. Karachentseva, Yu. N. Kudrya, and S. L. Parnovsky, Astronomy Letters **23**, 573 (1997).
 20. Yu. N. Kudrya, I. D. Karachentsev, V. E. Karachentseva, and S. L. Parnovskii, Astronomy Letters **23**, 11 (1997).
 21. M. Schmidt, Astrophys. J. **151**, 393 (1968).
 22. R. Giovanelli, E. Avera, and I. Karachentsev, Astronom. J. **114**, 122 (1997).
 23. D. I. Makarov, A. N. Burenkov, and N. V. Tyurina, Astronomy Letters **27**, 213 (2001).
 24. W. K. Huchtmeier, I. D. Karachentsev, V. E. Karachentseva, et al., Astronom. and Astrophys. **435**, 459 (2005).
 25. S. N. Mitronova, W. K. Huchtmeier, I. D. Karachentsev, et al., Astronomy Letters **31**, 501 (2005).
 26. I. D. Karachentsev and D. I. Makarov, Astrophysical Bulletin **63**, 299 (2008).
 27. D. Makarov and I. Karachentsev, Monthly Notices Roy. Astronom. Soc. **412**, 2498 (2011).
 28. A. Sandage, Astrophys. J. **307**, 1 (1986).